Supporting Information

Oriented self-assembly of metal-organic frameworks driven by photoinitiated monomer polymerization

Fuqiang Fan*, Zhihui Zhang, Qingqi Zeng, Liying Zhang, Xuemin Zhang, Tieqiang Wang and Yu Fu*

Department of Chemistry, College of Sciences, Northeastern University, Shenyang, 110819, P. R. China.
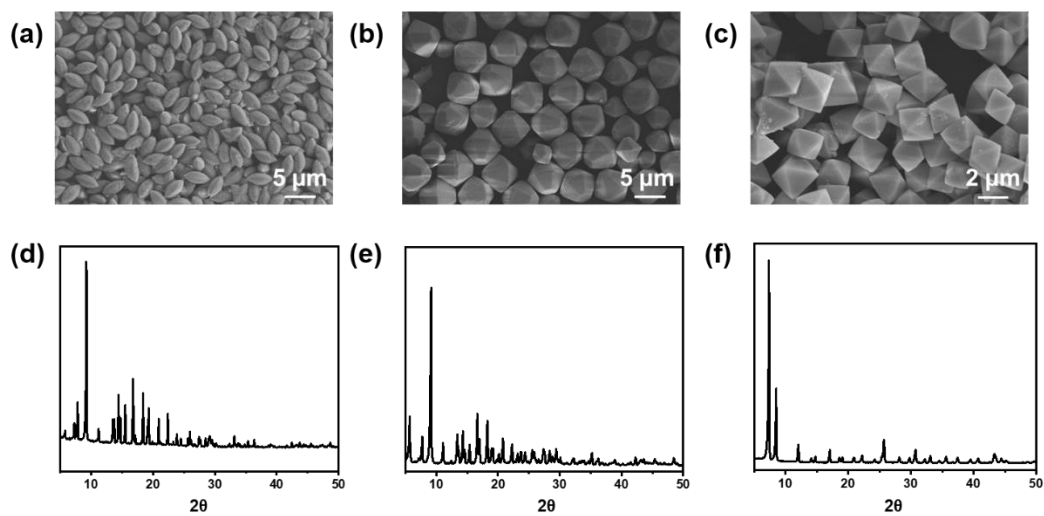
Figure S1. SEM images and PXRD patterns of the MOF particles. (a, d) MIL-96 spindle morphology; (b, e) MIL-96 hexagonal bifrustum morphology; (c, f) UIO-66 octahedral morphology.
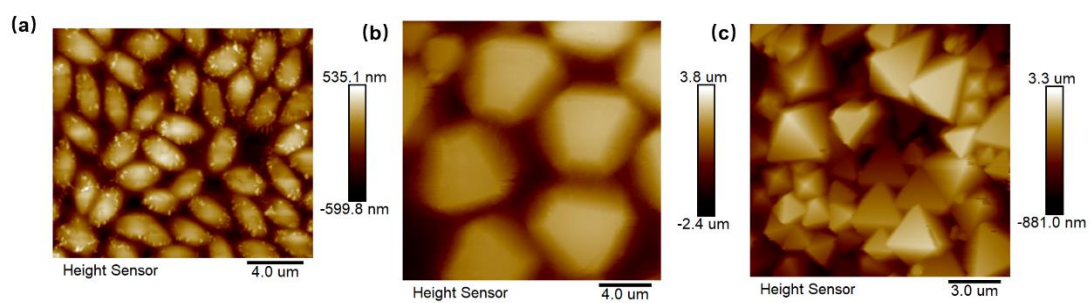
Figure S2. AFM images of the MOF films. (a) MIL-96 spindle morphology; (b) MIL-96 hexagonal bifrustum morphology; (c) UIO-66 octahedral morphology.

Table S1. (a) Crystallographic preferred orientation (CPO) index equation. If the CPO value is >1, it means the MOF material show a preferred orientation in crystal plane. (b) CPO values of MOF film fabricated using CH_2Cl_2 as the casting solvent.

(a)

$$CPO\frac{(X)}{(Y)} = \frac{\left(\frac{I_F^{(X)}}{I_F^{(Y)}}\right) - \left(\frac{I_P^{(X)}}{I_P^{(Y)}}\right)}{\left(\frac{I_P^{(X)}}{I_P^{(Y)}}\right)}$$

I: intensity of reflection of X or Y

F: film

P: power

(b)

CPO (X/Y)	UIO-66 polymer film
CPO (111/200)	2.15
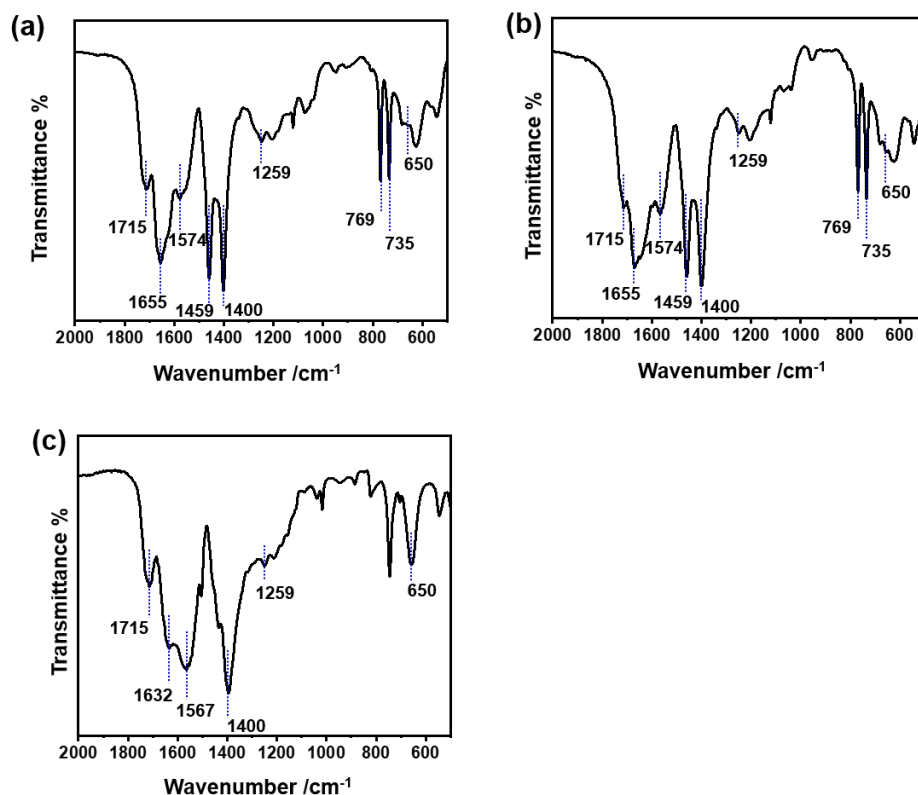
Figure S3. FT-IR spectrum of the MOF films. (a) MIL-96 spindle morphology; (b) MIL-96 hexagonal bifrustum morphology; (c) UIO-66 octahedral morphology.

The samples (a) and (b) were both composited of MIL-96 and polymer, resulting in the similar IR peaks. The vibration absorption of C=O at 1712 cm^{-1} and 1259 cm^{-1} of C-N belongs to polyurethane; 1655 cm^{-1} and 1574 cm^{-1} can be assigned to symmetric stretching, whereas the peaks at 1459 cm^{-1} and 1400 cm^{-1} belongs to symmetric stretching of carbonyl group; the band at 756 cm^{-1} and 735 cm^{-1} are ascribed to the C-H bending vibration in the aromatic ring; the band at 650 cm^{-1} belongs to the disulfide bonds. The peaks at 1632 cm^{-1} and 1567 cm^{-1} in sample (c) are assigned to symmetric stretching of carbonyl group.
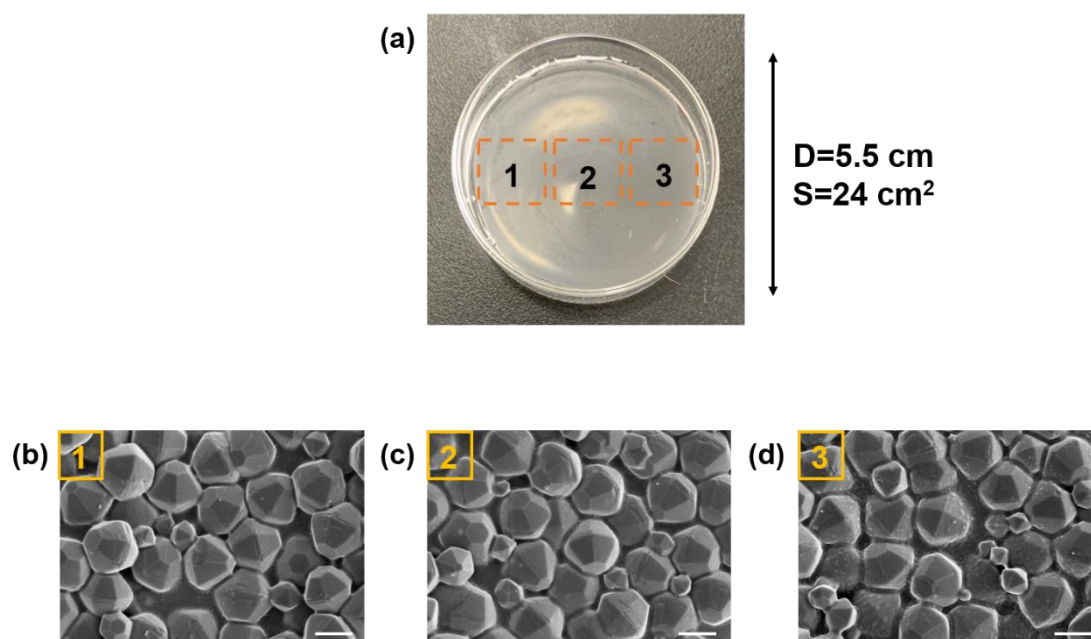
Figure S4. (a) Photograph of hexagonal bifrustum MIL-96 prepared by CH_2Cl_2 as the casting solvent. (b-d) SEM images of MOF film sampled at three different positions.
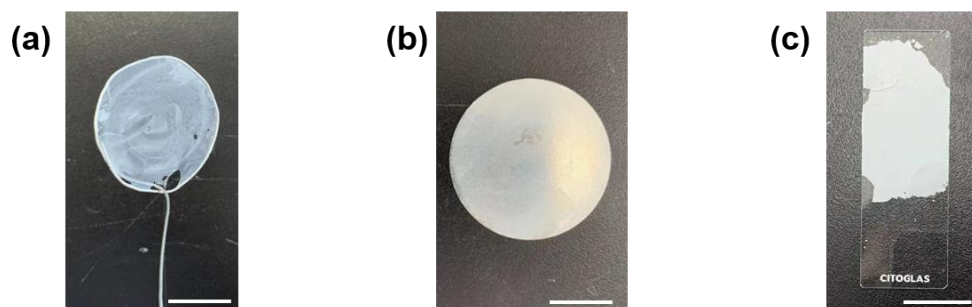
Figure S5. Photographs of hexagonal bifrustum MIL-96 films prepared by CH_2Cl_2 as free-standing (a), or transferred to Al foil (b) and glass (c).

Table S2. Properties of casting solvents.

Solvent	Density (g/cm³)	Boiling Point (℃)	Interfacial tension (mN/m)
THF	0.888	66	-
DMSO	1.1	189	-
Ethyl acetate	0.9	77.2	54
CH_2Cl_2	1.325	39.75	56
$CHCl_3$	1.428	61.2	66
Toluene	0.872	110.6	76
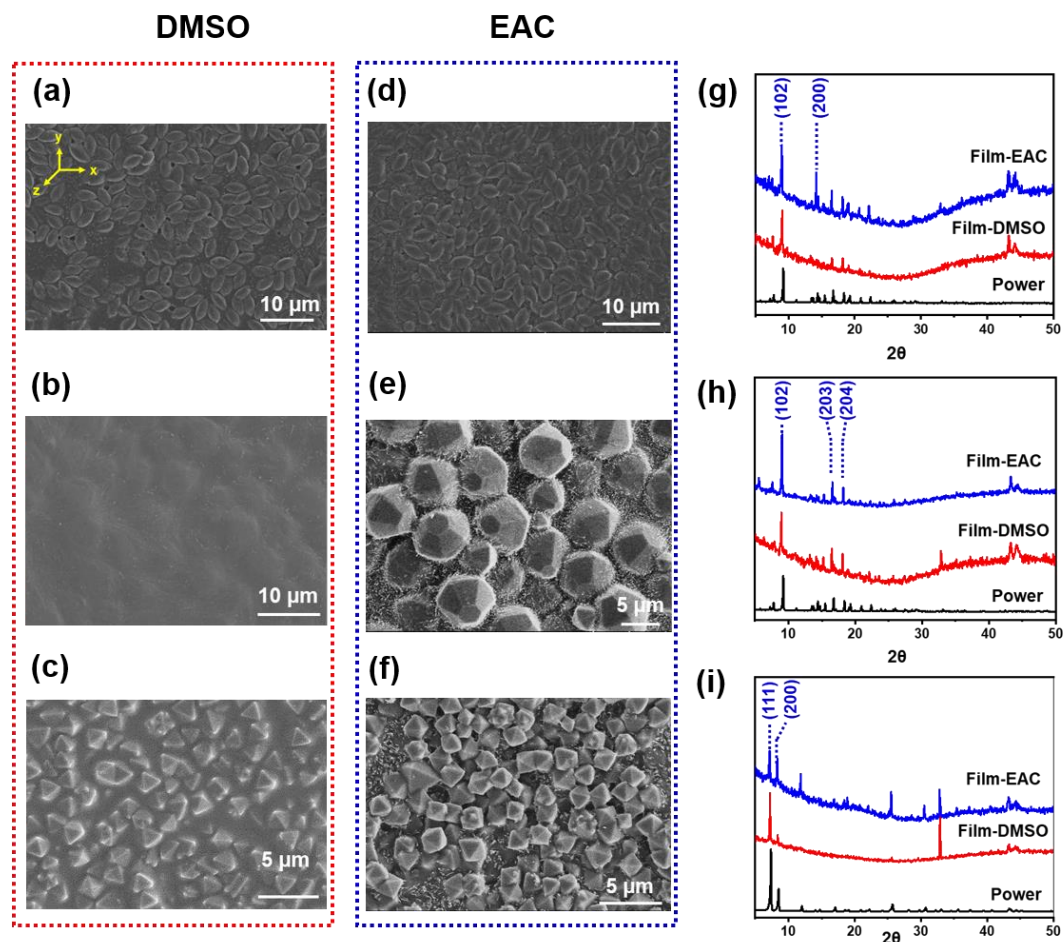
Figure S6. SEM images of the bottom surface of MIL-96 spindle morphology film, MIL-96 hexagonal bifrustum morphology film, UIO-66 octahedral morphology film prepared using different solvent: (a-c) DMSO; (d-f) EAC. PXRD patterns of the film using different MOF and solvents: (g) spindle morphology of MIL-96; (h) hexagonal bifrustum morphology of MIL-96; (i) octahedral morphology of UIO-66.

Table S3. CPO values of MOF films fabricated using different casting solvents.

CPO (X/Y)	Solvent	UIO-66 polymer film
CPO (200/111)	EAC	0.589
CPO (111/200)	CHCl$_3$	1.55
CPO (111/200)	THF	21
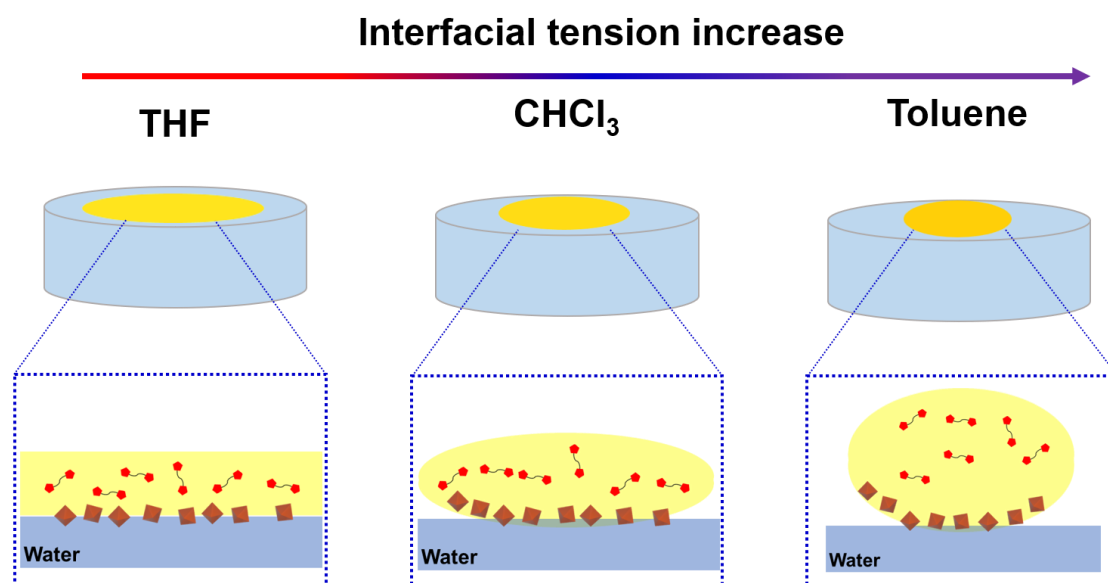
Figure S7. Schematic illustration of the alignment of the MOF particles at different water-liquid interface.
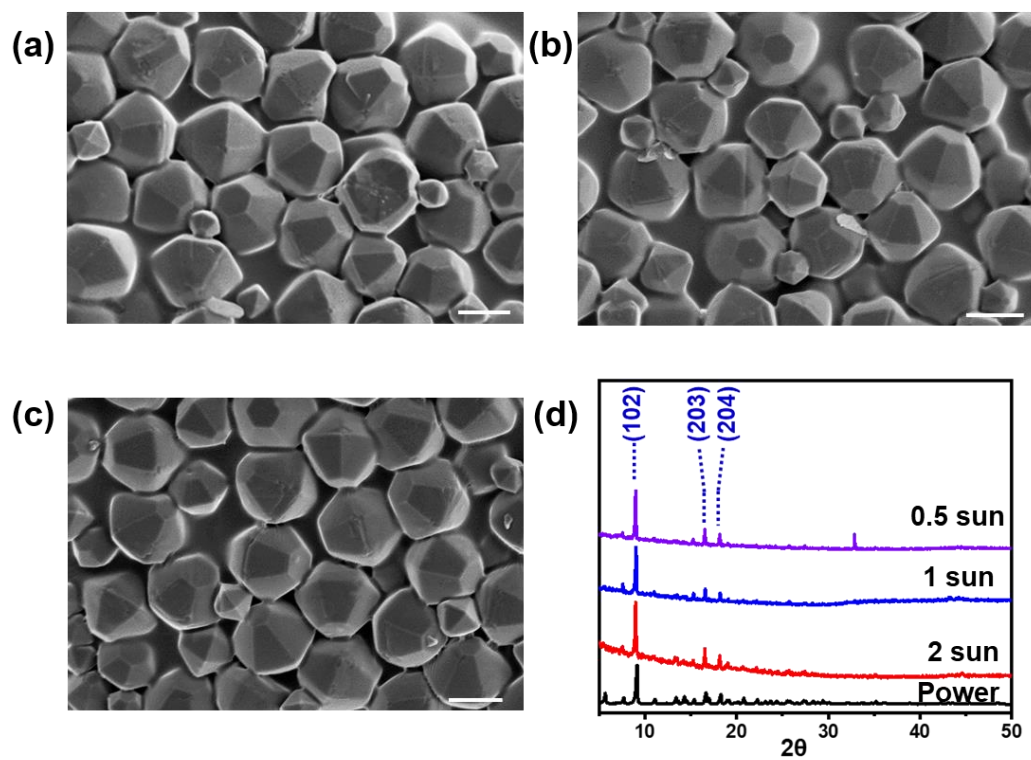
Figure S8. The SEM images of the MOF films prepared under different intensity of visible light. (a) 0.5 sun; (b) 1 sun; (c) 2 sun. (d) PXRD patterns of the MOF films. The intensity of 1 sun is nearly 1 kW m^{-2}.